A Finite Element Formulation for the Determination of Unknown Boundary Conditions for 3-D Steady Thermoelastic Problems

Brian H. Dennis

Institute of Environmental Studies,

The University of Tokyo,

7-3-1 Hongo, Bunkyo-ku,Tokyo, Japan 113-8656

e-mail: dennis@garlic.q.t.u-tokyo.ac.jp

George S. Dulikravich

Department of Mechanical and Aerospace Engineering,

The University of Texas at Arlington,

UTA Box 19018, Arlington, TX, U.S.A. 76019-0018

e-mail: dulikra@mae.uta.edu

Shinobu Yoshimura

Institute of Environmental Studies,

The University of Tokyo,

7-3-1 Hongo, Bunkyo-ku,Tokyo, Japan 113-8656

e-mail: yoshi@q.t.u-tokyo.ac.jp

ABSTRACT

A 3-D finite element method (FEM) formulation for the prediction of unknown boundary conditions in linear steady thermoelastic continuum problems is presented. The present FEM formulation is capable of determining displacements, surface stresses, temperatures, and heat fluxes on the boundaries where such quantities are unknown or inaccessible, provided such quantities are sufficiently over-specified on other boundaries. The method can also handle multiple material domains and multiply connected domains with ease. A regularized form of the method is also presented. The regularization is necessary for solving problems where the over-specified boundary data contain errors. Several regularization approaches are shown. The inverse FEM method described is an extension of a method previously developed by the leading authors for 2-D steady thermoelastic inverse problems and 3-D thermal inverse problems. The method is demonstrated for several 3-D test cases involving simple geometries although it is applicable to arbitrary 3-D configurations. Several different solution techniques for sparse rectangular systems are briefly discussed.

NOMENCLATURE

α	Coefficient of thermal expansion
$\{\delta\}$	Displacement vector
ϵ	strain
Γ	Boundary surface
λ	Lame's constant
Λ	Damping parameter
ν	Poisson's ratio

σ	Normal stress
$\bar{\sigma}$	Standard deviation
τ	Shear stress
Θ	Temperature
$\Delta\Theta$	difference between local and reference temperature
$[D]$	Damping matrix
E	Elastic modulus of elasticity
G	Shear modulus
k	Fourier coefficient of heat conduction
Q	Heat source
q	Heat flux
R	Uniform random number between 0 and 1
$\hat{n}$	Unit normal vector
u, v, w	Deformations in the x, y, z directions
X, Y, Z	Body force in x, y, z directions
x, y, z	Cartesian body axes

INTRODUCTION

It is often difficult or even impossible to place temperature probes, heat flux probes, or strain gauges on certain parts of a surface of a solid body. This can be due to its small size, geometric inaccessibility, or a exposure to a hostile environment. With an appropriate inverse method these unknown boundary values can be determined from additional information provided at the boundaries where the values can be measured directly. In the case of steady thermal and elastic problems, the objective of the inverse problem is to determine displacements, surface stresses, heat fluxes, and temperatures on boundaries where they are unknown. The problem of inverse determination of unknown boundary conditions in two-dimensional steady heat conduction has been solved by a variety of methods [1, 2, 3, 4, 5]. Similarly, a separate inverse boundary condition determination problem in linear elastostatics has been solved by different methods [6]. The inverse boundary condition determination problem for steady thermoelasticity was also solved for several two-dimensional problems [4].

A 3-D finite element formulation is presented here that allows one to solve this inverse problem in a direct manner by over-specifying boundary conditions on boundaries where that information is available. Our objective is to develop and demonstrate an approach for the prediction of thermal boundary conditions on parts of a three-dimensional solid body surface by using FEM.

It should be pointed out that the method for the solution of inverse problems to be discussed in this paper is different from the approach based on boundary element method that has been used separately in linear heat conduction [3] and linear elasticity [6].

For inverse problems, the unknown boundary conditions on parts of the boundary can be determined by overspecifying the boundary conditions (enforcing both Dirichlet and Neumann type boundary conditions) on at least some of the remaining portions of the boundary, and providing either Dirichlet or Neumann type boundary conditions on the rest of the boundary. It is possible, after a series of algebraic manipulations, to transform the original system of equations into a system which enforces the overspecified boundary conditions and includes the unknown boundary conditions as a part of the unknown solution vector. This formulation is an adaptation of a method used by Martin and Dulikravich [7] for the inverse detection of boundary conditions in steady heat conduction.

Specifically, this work represents an extension of the conceptual work presented by the authors [4, 8] by extending the original formulation from two dimensions into three dimensions.

FEM FORMULATION FOR THERMOELASTICITY

The Navier equations for linear static deformations u, v, w in three-dimensional Cartesian x, y, z coordinates are

$$(\lambda + G) \quad (\tfrac{\partial^2 u}{\partial x^2} + \tfrac{\partial^2 v}{\partial x \partial y} + \tfrac{\partial^2 w}{\partial x \partial z}) + G\nabla^2 u + X = \quad 0 \tag{1}$$

$$(\lambda + G) \quad (\tfrac{\partial^2 u}{\partial x \partial y} + \tfrac{\partial^2 v}{\partial y^2} + \tfrac{\partial^2 w}{\partial y \partial z}) + G\nabla^2 v + Y = \quad 0 \tag{2}$$

$$(\lambda + G) \quad (\tfrac{\partial^2 u}{\partial x \partial z} + \tfrac{\partial^2 v}{\partial y \partial z} + \tfrac{\partial^2 w}{\partial z^2}) + G\nabla^2 w + Z = \quad 0 \tag{3}$$

where,

$$\lambda = \frac{E\nu}{(1+\nu)(1-2\nu)}, \quad G = \frac{E}{2(1+\nu)}$$

Here, X, Y, Z are body forces per unit volume due to stresses from thermal expansion.

$$X = -(3\lambda + 2G)\frac{\partial \alpha \Delta \Theta}{\partial x} \tag{4}$$

$$Y = -(3\lambda + 2G)\frac{\partial \alpha \Delta \Theta}{\partial y} \tag{5}$$

$$Z = -(3\lambda + 2G)\frac{\partial \alpha \Delta \Theta}{\partial z} \tag{6}$$

This system of differential equations (1)-(3) can be written in the following matrix form

$$[L]^T([C][L]\{\delta\} - [C]\{\varepsilon_0\}) - \{f_b\} = 0 \tag{7}$$

where the differential operator matrix, $[L]$, is defined as

$$[L] = \begin{bmatrix} \frac{\partial}{\partial x} & 0 & 0 \\ 0 & \frac{\partial}{\partial y} & 0 \\ 0 & 0 & \frac{\partial}{\partial z} \\ \frac{\partial}{\partial y} & \frac{\partial}{\partial x} & 0 \\ \frac{\partial}{\partial z} & 0 & \frac{\partial}{\partial x} \\ 0 & \frac{\partial}{\partial z} & \frac{\partial}{\partial y} \end{bmatrix} \tag{8}$$

and the elastic modulus matrix, $[C]$, is defined as

$$[C] = \frac{\lambda}{\nu}\begin{bmatrix} 1-\nu & \nu & \nu & 0 & 0 & 0 \\ \nu & 1-\nu & \nu & 0 & 0 & 0 \\ \nu & \nu & 1-\nu & 0 & 0 & 0 \\ 0 & 0 & 0 & \frac{1-2\nu}{2} & 0 & 0 \\ 0 & 0 & 0 & 0 & \frac{1-2\nu}{2} & 0 \\ 0 & 0 & 0 & 0 & 0 & \frac{1-2\nu}{2} \end{bmatrix} \tag{9}$$

Casting the system of equations (7) in integral form using the weighted residual method [9, 10] yields

$$\int_\Omega [V][L]^T([C][L]\{\delta\} - [C]\{\varepsilon_0\})\, d\Omega - \int_\Omega [V]\{f_b\}\, d\Omega = 0 \tag{10}$$

where the matrix, $[V]$, is the weight matrix which is a collection of test functions.

$$[V] = \begin{bmatrix} v_1 & 0 & 0 \\ 0 & v_2 & 0 \\ 0 & 0 & v_3 \end{bmatrix} \tag{11}$$

One should now integrate (10) by parts to get the weak form of (7)

$$\int_\Omega ([L][V]^T)^T[C][L]\{\delta\}\, d\Omega - \int_\Omega ([L][V]^T)^T[C]\{\varepsilon_0\}\, d\Omega - \int_\Omega [V]\{f_b\}\, d\Omega - \int_{\Gamma_1} [V]\{T\}\, d\Gamma = 0 \tag{12}$$

where $\{T\}$ is the vector of surface tractions on surface Γ_1.

$$\{T\} = [n][C][L]\{\delta\} \tag{13}$$

The matrix $[n]$ contains the Cartesian components of the unit vector normal to the surface Γ_1. The displacement field in the x, y, and z directions can now be represented with approximation functions

$$\delta_x(x,y,z) \approx \tilde{\delta}_x^e(x,y,z) = \sum_{i=1}^{n} N_i(x,y,z)u_i \tag{14}$$

$$\delta_y(x,y,z) \approx \tilde{\delta}_y^e(x,y,z) = \sum_{i=1}^{n} N_i(x,y,z)v_i \tag{15}$$

$$\delta_z(x,y,z) \approx \tilde{\delta}_z^e(x,y,z) = \sum_{i=1}^{n} N_i(x,y,z)w_i \tag{16}$$

Equations (14)-(16) can be rewritten in matrix form

$$\tilde{\delta}^e = [N]\{\delta^e\} \tag{17}$$

where $[N]$ is the interpolation matrix which contains the trial functions for each equation in the system. Also note that with Galerkin's method the weight matrix and the interpolation matrix are equal, $[N] = [V]^T$. If the matrix $[B_e]$ is defined as

$$[B_e] = [L][N] \tag{18}$$

then the substitution of the approximation functions (17) into the weak statement (12) creates the weak integral form for a finite element expressed as

$$\begin{aligned}\int_{\Omega^e} [B_e]^T[C][B_e]\{\delta^e\}\, d\Omega^e - \int_{\Omega^e} [B_e]^T[C]\{\varepsilon_0^e\}\, d\Omega^e \\ - \int_{\Omega^e} [N]^T\{f_b^e\}\, d\Omega^e - \int_{\Gamma_1^e} [N]^T\{T^e\}\, d\Gamma^e = 0\end{aligned} \tag{19}$$

This can also be written in the matrix form as

$$[K^e]\{\delta^e\} = \{f^e\} \tag{20}$$

For thermal stresses, the initial elemental strain vector, ε_0^e, becomes

$$\{\varepsilon_0^e\} = \begin{bmatrix} \alpha\Delta\Theta & \alpha\Delta\Theta & \alpha\Delta\Theta & 0 & 0 & 0 \end{bmatrix}^T \tag{21}$$

The local stiffness matrix, $[K^e]$, and the force per unit volume vector, $\{f^e\}$, are determined for each element in the domain and then assembled into the global system

$$[K]\{\delta\} = \{F\} \tag{22}$$

After applying boundary conditions, the global displacements are found by solving this system of linear algebraic equations. The stresses, $\{\sigma\}$, can then be found in terms of the displacements, $\{\delta\}$

$$\{\sigma\} = [C][L]\{\delta\} - [C]\{\varepsilon_0\} \tag{23}$$

FEM FORMULATION FOR THE THERMAL PROBLEM

The temperature distribution throughout the domain can be found by solving Poisson's equation for steady linear heat conduction with a distributed steady heat source function, Q, and thermal conductivity coefficient, k.

$$-k\left(\frac{\partial^2\Theta}{\partial x^2} + \frac{\partial^2\Theta}{\partial y^2} + \frac{\partial^2\Theta}{\partial z^2}\right) = Q \tag{24}$$

Applying the method of weighted residuals to (24) over an element results in

$$\int_{\Omega^e} \left(\frac{\partial^2\Theta}{\partial x^2} + \frac{\partial^2\Theta}{\partial y^2} + \frac{\partial^2\Theta}{\partial z^2} - \frac{Q}{k}\right) v\, d\Omega^e = 0 \tag{25}$$

Integrating this by parts once (25) creates the weak statement for an element

$$\begin{aligned}-\int_{\Omega^e} k\left(\frac{\partial v}{\partial x}\frac{\partial\Theta}{\partial x} + \frac{\partial v}{\partial y}\frac{\partial\Theta}{\partial y} + \frac{\partial v}{\partial z}\frac{\partial\Theta}{\partial z}\right) d\Omega^e \\ = \int_{\Omega^e} N_i Q\, d\Omega^e - \int_{\Gamma^e} N_i (q\cdot\hat{n})\, d\Omega^e\end{aligned} \tag{26}$$

Variation of the temperature across an element can be expressed by

$$\Theta(x,y,z) \approx \tilde{\Theta}^e(x,y,z) = \sum_{i=1}^{m} N_i(x,y,z)\Theta_i \tag{27}$$

Using Galerkin's method, the weight function v and the interpolation function for Θ are chosen to be the same.
By defining the matrix $[B_T]$ as

$$[B_T] = \begin{bmatrix} \frac{\partial N_1}{\partial x} & \frac{\partial N_2}{\partial x} & \cdots & \frac{\partial N_m}{\partial x} \\ \frac{\partial N_1}{\partial y} & \frac{\partial N_2}{\partial y} & \cdots & \frac{\partial N_m}{\partial y} \\ \frac{\partial N_1}{\partial z} & \frac{\partial N_2}{\partial z} & \cdots & \frac{\partial N_m}{\partial z} \end{bmatrix} \tag{28}$$

the weak statement (26) can be written in the matrix form as

$$[K_c^e]\{\Theta^e\} = \{Q^e\} \tag{29}$$

where

$$[K_c^e] = \int_{\Omega^e} k[B_T]^T[B_T]\, d\Omega^e \tag{30}$$

$$\{Q^e\} = -\int_{\Omega^e} Q\{N\}\, d\Omega + \int_{\Gamma^e} q_s\{N\}\, d\Gamma^e \tag{31}$$

The local stiffness matrix, $[K_c^e]$, and heat flux vector, $\{Q^e\}$, are determined for each element in the domain and then assembled into the global system

$$[K_c]\{\Theta\} = \{Q\} \tag{32}$$

DIRECT AND INVERSE FORMULATIONS

The above equations for steady thermoelasticity were discretized by using a Galerkin's finite element method. This results in two linear systems of algebraic equations

$$[K]\{\delta\} = \{F\}, \quad [K_c]\{\Theta\} = \{Q\} \tag{33}$$

The system is typically large, sparse, symmetric, and positive definite. Once the global system has been formed, the boundary conditions are applied. For a well-posed analysis (direct) problem, the boundary conditions must be known on all boundaries of the domain. For heat conduction, either the temperature, Θ_s, or the heat flux, Q_s, must be specified at each point of the boundary.

For an inverse problem, the unknown boundary conditions on parts of the boundary can be determined by over-specifying the boundary conditions (enforcing both Dirichlet and Neumann type boundary conditions) on at least some of the remaining portions of the boundary, and providing either Dirichlet or Neumann type boundary conditions on the rest of the boundary. It is possible, after a series of algebraic manipulations, to transform the original system of equations into a system which enforces the over-specified boundary conditions and includes the unknown boundary conditions as a part of the unknown solution vector. As an example, consider the linear system for heat conduction on a tetrahedral finite element with boundary conditions given at nodes 1 and 4.

$$\begin{bmatrix} K_{11} & K_{12} & K_{13} & K_{14} \\ K_{21} & K_{22} & K_{23} & K_{24} \\ K_{31} & K_{32} & K_{33} & K_{34} \\ K_{41} & K_{42} & K_{43} & K_{44} \end{bmatrix} \begin{Bmatrix} \Theta_1 \\ \Theta_2 \\ \Theta_3 \\ \Theta_4 \end{Bmatrix} = \begin{Bmatrix} Q_1 \\ Q_2 \\ Q_3 \\ Q_4 \end{Bmatrix} \tag{34}$$

As an example of an inverse problem, one could specify both the temperature, Θ_s, and the heat flux, Q_s, at node 1, flux only at nodes 2 and 3, and assume the boundary conditions at node 4 as being unknown. The original system of equations (34) can be modified by adding a row and a column corresponding to the additional equation for the over-specified flux at node 1 and the additional unknown due to the unknown boundary flux at node 4. The result is

$$\begin{bmatrix} 1 & 0 & 0 & 0 & 0 \\ K_{21} & K_{22} & K_{23} & K_{24} & 0 \\ K_{31} & K_{32} & K_{33} & K_{34} & 0 \\ K_{41} & K_{42} & K_{43} & K_{44} & -1 \\ K_{11} & K_{12} & K_{13} & K_{14} & 0 \end{bmatrix} \begin{Bmatrix} \Theta_1 \\ \Theta_2 \\ \Theta_3 \\ \Theta_4 \\ Q_4 \end{Bmatrix} = \begin{Bmatrix} \Theta_s \\ Q_2 \\ Q_3 \\ 0 \\ Q_s \end{Bmatrix} \tag{35}$$

The resulting systems of equations will remain sparse, but will be non-symmetric and possibly rectangular (instead of square) depending on the ratio of the number of known to unknown boundary conditions.

REGULARIZATION

Three regularization methods were applied separately to the solution of the systems of equations in attempts to increase the method's tolerance for measurement errors in the over-specified boundary conditions. Here we consider the regularization of the inverse heat conduction problem.

The general form of a regularized system is given as [11]:

$$\left[\begin{array}{c} K_c \\ \Lambda D \end{array} \right] \{\Theta\} = \left\{ \begin{array}{c} Q \\ 0 \end{array} \right\} \tag{36}$$

The traditional Tikhonov regularization is obtained when the damping matrix, $[D]$, is set equal to the identity matrix. Solving (36) in a least squares sense minimizes the following error function.

$$error(\Theta) = |||[K_c]\{\Theta\} - \{Q\}||_2^2 + ||\Lambda[D]\{\Theta\}||_2^2 \tag{37}$$

This is the minimization of the residual plus a penalty term. The form of the damping matrix determines what penalty is used and the damping parameter, Λ, weights the penalty for each equation. These weights should be determined according to the error associated with the respective equation.

Method 1

This method of regularization uses a constant damping parameter Λ over the entire domain and the identity matrix as the damping matrix. This method can be considered the traditional "zeroth order" Tikhonov method. The penalty term being minimized in this case is the square of the L_2 norm of the solution vector $\{x\}$. Minimizing this norm will tend to drive the components of $\{x\}$ to uniform values thus producing a smoothing effect. However, minimizing this penalty term will ultimately drive each component to zero, completely destroying the real solution. Thus, great care must be exercised in choosing the damping parameter Λ so that a good balance of smoothness and accuracy is achieved.

Method 2

This method of regularization uses a constant damping parameter Λ only for equations corresponding to the unknown boundary values. For all other equations $\Lambda = 0$ and $[D] = [I]$ since the largest errors occur at the boundaries where the temperatures and fluxes are unknown.

Method 3

This method uses Laplacian smoothing of the unknown temperatures and displacements only on the boundaries where the boundary conditions are unknown. This method could be considered a "second order" Tikhonov method. A penalty term can be constructed such that curvature of the solution on the unspecified boundary is minimized along with the residual.

$$||\nabla^2 \Theta_{ub}||_2^2 \rightarrow \min \tag{38}$$

For problems that involve unknown vector fields, such as displacements, Eqn. (38) must be modified to the following.

$$||\nabla^2 (\hat{n} \cdot \{\delta_{ub}\})||_2^2 \rightarrow \min \tag{39}$$

Here the normal component of the vector displacement field $\{\delta\}$ is minimized along the unknown surface.

Eqns. (38) and (39) can be discretized using the method of weighted residuals to determine the damping matrix, $[D]$.

$$|||[D]\Theta_{ub}||_2^2 = |||[K_c]\Theta_{ub}||_2^2 \tag{40}$$

In three-dimensional problems, $[K_c]$ is computed by integrating over surface elements on the unknown boundaries. So the damping matrix can be thought of as an assembly of boundary elements that make up the boundary of the object where the boundary conditions are unknown. The stiffness matrix for each boundary element is formed by using a Galerkin weighted residual method that ensures the Laplacian of the solution is minimized over the unknown boundary surface. The main advantage of this method is its ability to smooth the solution vector without necessarily driving the components to zero and away from the true solution.

SOLUTION OF THE LINEAR SYSTEM

In general, the resulting FEM systems for inverse thermoelastic problems are sparse, unsymmetric, and often rectangular. These properties make the process of finding a solution to the system very challenging. Three approaches will be discussed here.

The first is to normalize the equations by multiplying both sides by the matrix transpose and solve the resulting square system with common sparse solvers.

$$[K]^T[K]\{\Theta\} = [K]^T\{Q\} \tag{41}$$

This approach has been found to be effective for certain inverse problems [12]. The resulting normalized system is less sparse than the original system, but it is square, symmetric, and positive definite with application of regularization. The normalized system is solved with a direct method (Cholesky or LU factorization) or with a ILU preconditioned iterative method (preconditioned Krylov subspace). There are several disadvantages to this approach. Among them being the expense of computing $[K]^T[K]$, the large in-core memory requirements, and the roundoff error incurred during the $[K]^T[K]$ multiplication. In general, it is best to avoid methods that require the explicit of formation of $[K]^T[K]$.

Another approach is to use iterative methods suitable for least squares problems. One such method is the LSQR method, which is an extension of the well-known conjugate gradient (CG) method [13]. The LSQR method and other similar methods such as the conjugate gradient for least squares (CGLS) solve the normalized system, but without explicit computation of $[K]^T[K]$. These methods need only matrix-vector products at each iteration and therefore only require the storage of $[K]$ so they are attractive for large sized models. However, convergence rates of these methods depend strongly on the condition number of the normalized system which is the condition number of $[K]$ squared [14]. Therefore, solver performance degrades significantly as the size of the finite element model increases. Convergence can be slow when solving the systems resulting from the inverse finite element discretization since they are naturally ill-conditioned problems.

Yet another approach is to use a non-iterative method for least squares problems such as QR factorization [15] or SVD [16]. However, sparse implementations of QR or SVD solvers are needed to reduce the in-core memory requirements for the inverse finite element problems. It is also possible to use static condensation to reduce the complete sparse system of equations into a dense matrix of smaller dimensions [5]. The reduced system involves only the unknowns on the boundary of the domain and can be solved efficiently using standard QR or SVD algorithms for dense matrices.

NUMERICAL RESULTS

The accuracy and efficiency of the finite element inverse formulation was tested on several simple three-dimensional problems. The method was implemented in an object-oriented finite element code written in C++. Elements used in the calculations were hexahedra with tri-linear interpolation functions. The linear systems were solved with a sparse QR factorization [15] or LSQR method [13] with column scaling. The two basic test geometries included an annular cylinder and a cylinder with multiply connected regions.

The annular cylinder geometry was tested first. The hexahedral mesh is shown in Figure 1. The outer surface has a radius of 3.0 and the inner surface has a radius of 2.0. The mesh is composed of 1440 elements and 1980 nodes. The inner and outer boundaries each have 396 nodes. For this geometry, there is an analytical solution for heat conduction if constant temperature boundary conditions are used on the inner and outer boundaries. In a direct (well-posed) thermoelastic problem a uniform temperature of 10.0 ^oC was enforced on the inner boundary while a temperature of -10.0 ^oC was enforced on the outer boundary. Zero displacement was enforced on the cylinder outer boundary. A uniform pressure of 1.0 Pa was specified on the inner boundary. The following material properties were used: $E = 1.0$ Pa, $\nu = 0.0$, $\alpha = 2.0 \times 10^{-2}$ K^{-1}, k = 1.0 W m^{-1}K^{-1}. Adiabatic and stress free conditions were specified at the ends of the cylinder. The computed temperature field and stress field is shown in Figures 2and 4. The temperature field computed with the FEM had a maximum error of less than 1.0% compared to the analytical solution.

The inverse problem was then created by over-specifying the outer cylindrical boundary with the double-precision values of temperatures, fluxes, displacements, and reaction forces on the outer boundary obtained from the direct analysis case. At the same time, no boundary conditions were specified on the inner cylindrical boundary [3]. A damping parameter of $\Lambda = 0.0$ was used. The computed temperature and normal stress magnitude distributions are shown in Figures 3 and 5. The maximum relative differences in temperatures and displacements between the analysis and inverse results are less than 0.1% when solved using the QR factorization [15].

The above problem was repeated for the thermal problem only using boundary conditions with random measurement errors added. For these cases, regularization was used. Random errors in the known boundary temperatures and fluxes were generated using the following equations [3]:

$$\Theta = \Theta_{bc} \pm \sqrt{-2\sigma^2 \ln R} \tag{42}$$

$$Q = Q_{bc} \pm \sqrt{-2\sigma^2 \ln R} \tag{43}$$

Here R is a uniform random number between 0.0 and 1.0 and σ is the standard deviation. For each case, Eqns. (42)-(43) were used to generate errors in both the known boundary fluxes and temperatures obtained from the forward solution.

First, regularization method 1 was used with a wide range of damping parameters. The average percent error of the predicted temperatures on the unknown boundaries as a function of damping parameter and various levels of measurement error is shown in Figure 6.

The inverse problem was also solved using regularization method 2 and method 3 for a wide range of damping parameters. The average percent error of the predicted temperatures on the unknown boundary as a function of damping parameter is shown in Figure 7 for method 2 and Figure 8 for method 3.

Results indicate that for simple 3-D geometries the present formulation is capable of predicting the unknown boundary conditions with errors on the same order of magnitude as the errors in the over-specified data. In other words, all regularization methods prevent the amplification of the measurement errors. Regularization method 2 achieved slightly more accurate results than method 1 for all levels of random measurement error. However, method 3 produced the most accurate results overall.

The lack of error amplification with this method may only occur for simple geometries. Results in 2-D indicate that more sophisticated regularization techniques like method 3 are necessary for complicated geometries such as multiply connected domains [4].

The next test case involved a multiply-connected domain. Heat conduction only is considered in order to give a clear comparison of regularization methods for a more complex geometry. The geometry is composed of an outer cylinder with length 5.0 m and diameter of 2.0 m. There are four cylindrical holes that pass completely through the cylinder, each with a diameter of 1.25 m. The hexahedral mesh is shown in Figure 9 and is composed of 1440 elements and 1980 nodes. The inner and outer boundaries each have 440 nodes. For this geometry, there is no analytical solution, even if constant temperature boundary conditions are used on the boundaries.

In the direct (well-posed) problem a uniform temperature of 10.0 ^oC was enforced on the inner boundaries while a temperature of -10.0 ^oC was enforced on the outer boundary. Adiabatic boundary conditions were specified at the ends of the cylinder. The computed temperature field is shown in Figure 10.

The inverse problem was then created by over-specifying the outer cylindrical boundary with the double-precision values of temperatures and fluxes obtained from the analysis case. At the same time, no boundary conditions were specified on the inner cylindrical boundaries. No errors were used in the over-specified boundary data.

A damping parameter of $\Lambda = 0$ was tried first. Without regularization, the QR factorization became unstable due to the high condition number of the linear system.

The same inverse problem was repeated using regularization method 1 for a wide range of damping parameters. The lowest percent error achieved was 9.97% at damping parameter value of $\Lambda = 1.75 \times 10^{-8}$. The resulting temperature distribution for $\Lambda = 1.75 \times 10^{-8}$ is shown in Figure 11.

The inverse problem was also solved using regularization method 2 for a wide range of damping parameters. The lowest percent error achieved was 2.67% at damping parameter value of $\Lambda = 1.75 \times 10^{-8}$. The resulting temperature distribution for $\Lambda = 1.75 \times 10^{-8}$ is shown in Figure 12.

Finally, the inverse problem was solved using regularization method 3. A value of $\Lambda = 0.1$ was used and percent error compared to the direct solution was less than 0.0001%. The resulting temperature distribution is shown in Figure 13.

For the multiply-connected domain case only regularization method 3 worked well. These results indicate that this FEM inverse method requires regularization that is more sophisticated than the regular Tikhonov method if high accuracy is needed with multiply-connected three-dimensional geometries.

The final test case involves solving the thermoelastic inverse problem for the multiply-connected domain in Figure 9. This case considers thermal and elastic boundary conditions that vary in all coordinate directions thereby creating a truly three-dimensional example. The all interior boundary conditions change linearly along the z-axis. The exact values used are given in Table 1. On the outer cylinder the displacement was set to zero and a fixed temperature of 10 ^oC was specified. The following material properties were used: $E = 1.0\ Pa$, $\nu = 0.0$, $\alpha = 2.0 \times 10^{-2}$ K^{-1}, k = 1.0 W m^{-1}K^{-1}.

The inverse problem was generated by over-specifying the outer cylindrical boundary with the double-precision values of temperatures, fluxes, displacements, and surface tractions obtained from the forward analysis case. At the same time, no boundary conditions were specified on the inner cylindrical boundaries. No errors were used in the over-specified boundary data.

Regularization method 3 was used with $\Lambda = 8.5 \times 10^{-5}$. Our experience indicates that a good value for the damping parameter, Λ, is geometry and boundary condition dependent. Currently, the damping parameter is chosen based on experience by first choosing a small value and gradually increasing it until the numerical oscillations in the unknown boundary solution are removed.

The system of equations for temperature was solved using sparse QR factorization. The linear system for displacements was too large to be solved with the sparse QR factorization code. Alternatively, the system was solved using the LSQR method with column scaling. The LSQR iterations were terminated after the Euclidean norm of the residual of the normal system was less than 1.0×10^{-6}. In this example 16805 LSQR iterations were required, which consumed about 10 minutes of computing time on a Pentium 4 workstation.

The average error between the inverse and direct solutions on the unknown boundaries was 0.02% for temperature and 5.6% for displacement. The direct and inverse temperature contours for three sections of the domain are shown in Figs. 14, 16, and 18. There is good agreement on all three sections between the direct and inverse temperature contours. The direct and inverse displacement magnitude contours for three sections of the domain are shown in Figs. 15, 17, and 19. For all three

sections there is a noticeable difference in the direct and inverse contours in the regions far away from the outer boundary. However, the inverse solution does correctly capture the direct solution in a qualitative sense.

This thermoelastic problem was also solved using the other regularization methods over a wide range of damping parameters. In those cases the error in the inverse solution was much higher and did not match the direct solution even in a qualitative sense. The accuracy of the displacement could be increased by improving the quality of the damping matrix for the displacement field. The current damping matrix of Method 3 from Eqn. 39 only includes the normal component of the displacement. Further improvements could be made by smoothing the tangential components as well. In addition, the current scheme depends on accurate surface unit normal vectors, $\hat{n}$, which are difficult to compute accurately on the nodes of flat elements on curved surfaces. So further reductions in errors could possibly be made by implementing methods that compute the surface normals with a high degree of accuracy.

The sparse QR factorization was found to provide the solution with highest accuracy in the shortest amount of computing time. However, the QR factorization requires substantial amounts of in-core memory. For the largest examples presented here, a workstation with 512 MB of memory was required. The sparse QR factorization failed for the elastic inverse problem on the multiply-connected domain that had more than 7,000 unknowns. For cases where QR factorization failed or required too much memory, the LSQR method was employed. Reasonable results were obtained by LSQR with column scaling in less than 20,000 iterations for displacements and 3,000 iterations for temperature. Although many iterations are required with the LSQR method, it requires much less memory and is more robust than the sparse QR factorization. The preconditioned CG method applied to the normalized equations worked well for problems with less than 100 nodes. For more than 100 nodes, this method required many iterations to converge to a solution less accurate than the QR or LSQR solution. When regularization was applied to the sparse matrix, the CG convergence improved dramatically but the QR factorization was much faster by comparison.

CONCLUSIONS

A formulation for the inverse determination of unknown steady boundary conditions in heat conduction and thermoelasticity for three-dimensional problems has been developed using FEM. The formulation has been tested numerically using an annular geometry with a known analytic solution. The formulation can predict the temperatures and displacements on the unknown boundary with high accuracy in the annular domain without the need for regularization. However, regularization was required in order to compute a good solution when measurement errors in the over-specified boundary conditions were added. Three different regularization methods were applied. All allow a stable QR factorization to be computed, but only method 3 resulted in highly accurate temperature predictions on the unknown boundaries for large values of measurement errors. However, all regularization methods prevented amplification of the measurement errors. It was shown that the FEM formulation can accurately predict unknown boundary conditions for multiply-connected domains when a good regularization scheme is used. Further research is needed to develop better regularization methods so that the present formulation can be made more robust with respect to measurement errors and more complex geometries. Further research is also needed to improve regularization for inverse problems in elasticity over complicated domains.

ACKNOWLEDGEMENTS

The primary author would like to acknowledge the support received from the ADVENTURE project sponsored by the Japanese Society for the Promotion of Science (JSPS) and the "Frontier Simulation Software for Industrial Science (FSIS)" project supported by IT program of Japan Ministry of Education, Culture, Sports, Science and Technology (MEXT).

REFERENCES

[1] Larsen, M.E. , 1985, "An Inverse Problem: Heat Flux and Temperature Prediction for a High Heat Flux Experiment," Tech. rep. SAND-85-2671, Sandia National Laboratories, Albuquerque, NM.

[2] Hensel, E. H. and Hills, R. , 1989, "Steady-State Two-Dimensional Inverse Heat Conduction," *Numerical Heat Transfer*, pp. pp. 227–240.

[3] Martin, T. J. and Dulikravich, G. S. , 1996, "Inverse Determination of Boundary Conditions in Steady Heat Conduction," *ASME Journal of Heat Transfer*, pp. pp. 546–554.

[4] Dennis, B. H. and Dulikravich, G. S. , 1999, "Simultaneous Determination of Temperatures, Heat Fluxes, Deformations, and Tractions on Inaccessible Boundaries," *ASME Journal of Heat Transfer*, pp. pp. 537–545.

[5] Olson, L. G. and Throne, R. D. , 2000, "The Steady Inverse Heat Conduction Problem: A Comparison for Methods of Inverse Parameter Selection," In *34th National Heat Transfer Conference-NHTC'00*, No. NHTC2000-12022, Pittsburg, PA.

[6] Martin, T. J. , Halderman, J. , and Dulikravich, G. S. , 1995, "An Inverse Method for Finding Unknown Surface Tractions and Deformations in Elastostatics," *Computers and Structures*, pp. pp. 825–836.

[7] Martin, T. J. and Dulikravich, G. S. , 1995, "Finding Temperatures and Heat Fluxes on Inaccessible Surfaces in 3-D Coated Rocket Nozzles," In *1995 JANNAF Non-Destructive Evaluation Propulsion Subcommittee Meeting*, Tampa, FL. pp. 119–129.

[8] Dennis, B. H. and Dulikravich, G. S. , 2001, "A 3-D Finite Element Formulation for the Determination of Unknown Boundary Conditions in Heat Conduction," In *Proc. of Internat. Symposium on Inverse Problems in Eng. Mechanics*, Tanaka, M. , editor, Nagano City, Japan.

[9] Hughes, T. J. R. , 2000, *The Finite Element Method: Linear Static and Dynamic Finite Element Analysis.* Dover Publications, Inc., New York.

[10] Huebner, K. H. , Thorton, E. A. , and Byrom, T. G. , 1995, *The Finite Element Method for Engineers.* John Wiley and Sons, New York, NY, third edition.

[11] Neumaier, A. , 1998, "Solving Ill-Conditioned and Singular Linear Systems: A Tutorial on Regularization," *SIAM Review*, pp. pp. 636–666.

[12] Boschi, L. and Fischer, R. P. , 1996, "Iterative Solutions for Tomographic Inverse Problems: LSQR and SIRT," Tech. Rep. Seismology Dept., Harvard University, Cambridge, MA.

[13] Paige, C. C. and Saunders, M. A. , 1982, "LSQR: An Algorithm for Sparse Linear Equations and Sparse Least Squares," *ACM Transactions on Mathematical Software*, pp. pp. 43–71.

[14] Saad, Y. , 1996, *Iterative Methods for Sparse Linear Systems.* PWS Publishing Co., Boston, MA.

[15] Matstoms, P. , 1991, *The multifrontal solution of sparse least squares problems*, PhD thesis, Linköping University, Sweden.

[16] Golub, G. H. and Van Loan, C. F. , 1996, *Matrix Computations.* Johns Hopkins University Press, Baltimore, MD.

TABLE 1: Temperature and pressure boundary conditions for interior surfaces

Hole	$T_{z=0}$ (^oC)	$T_{z=5}$ (^oC)	$P_{z=0}$ (Pa)	$P_{z=5}$ (Pa)
A	5.0	2.0	2.0	1.0
B	6.0	1.0	2.0	1.0
C	7.0	1.0	2.0	1.0
D	8.0	2.0	2.0	1.0

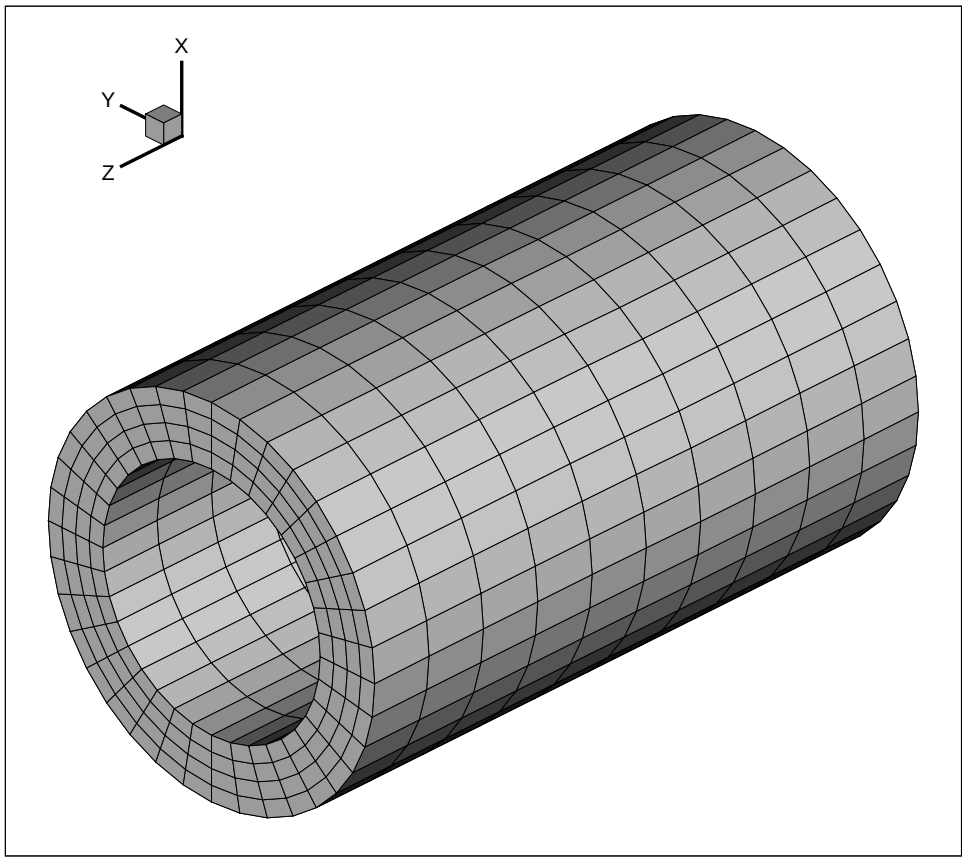

Figure 1: Surface mesh for cylinder test case

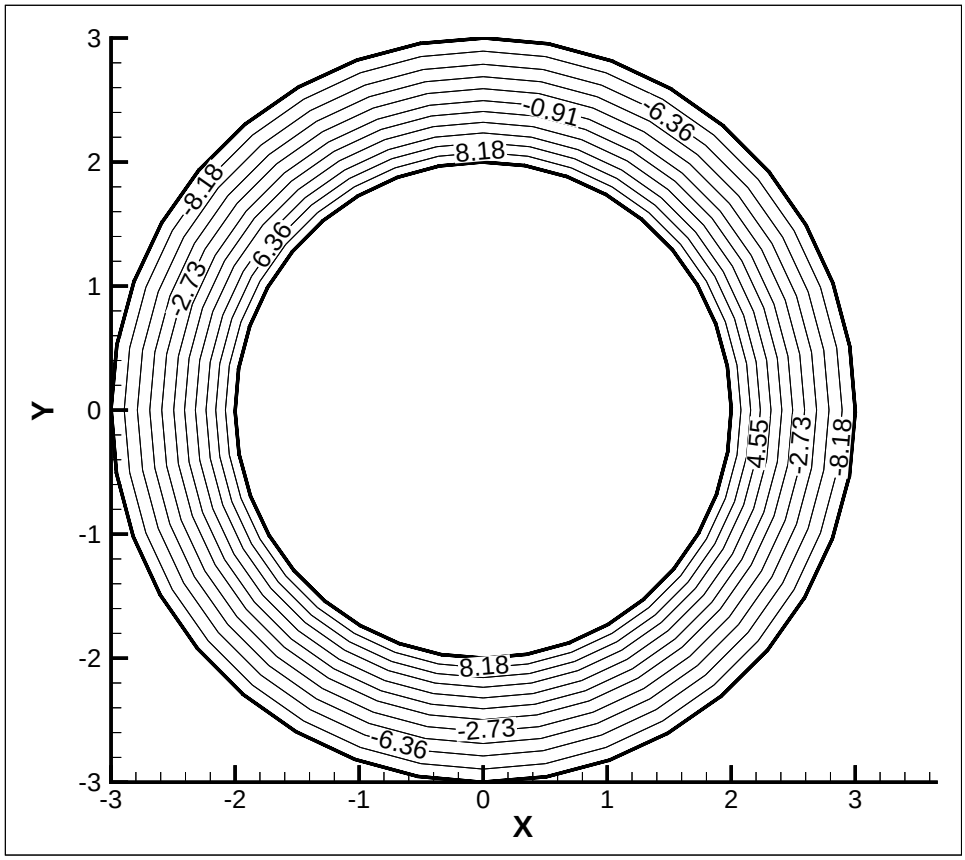

Figure 2: Direct problem: computed isotherms when both inner and outer boundary temperatures were specified

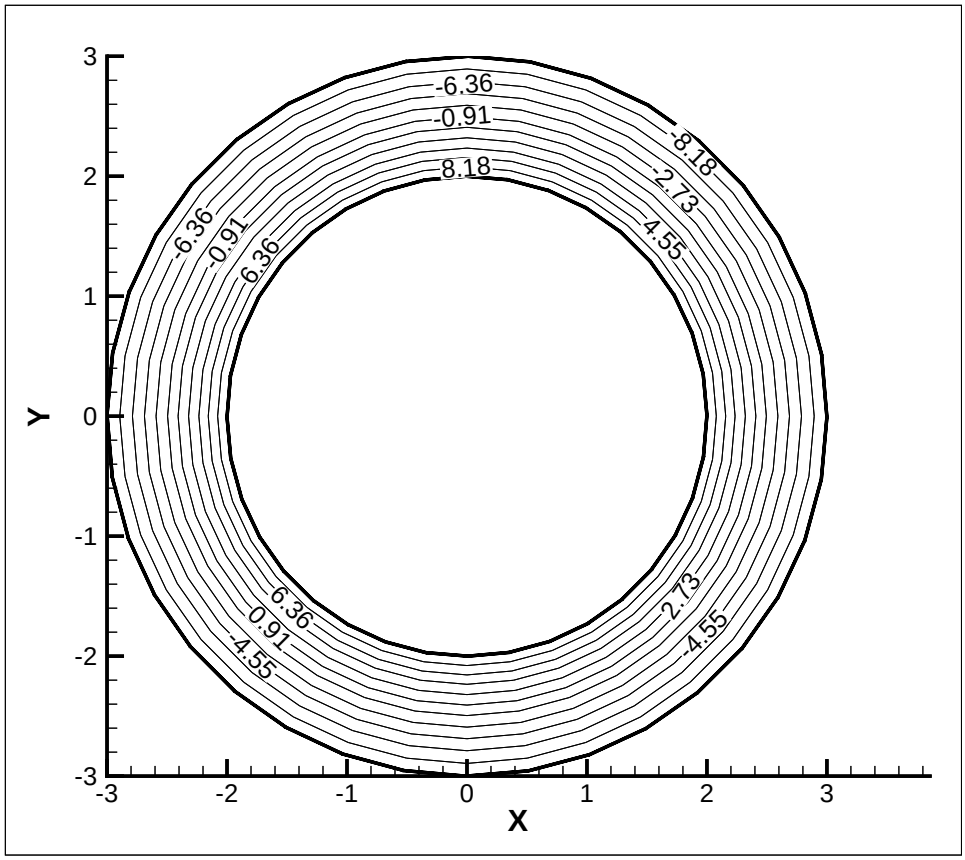

Figure 3: Inverse problem: computed isotherms when only outer boundary temperatures and fluxes were specified

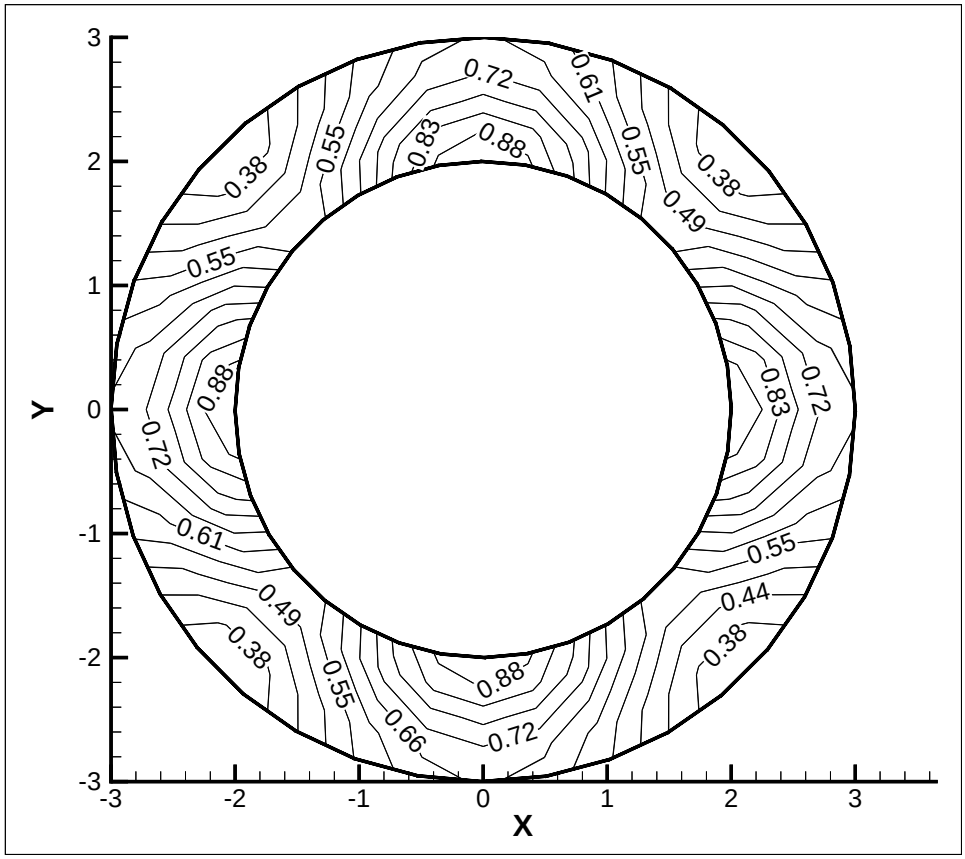

Figure 4: Direct problem: computed normal stress magnitude when both inner and outer boundary conditions were specified

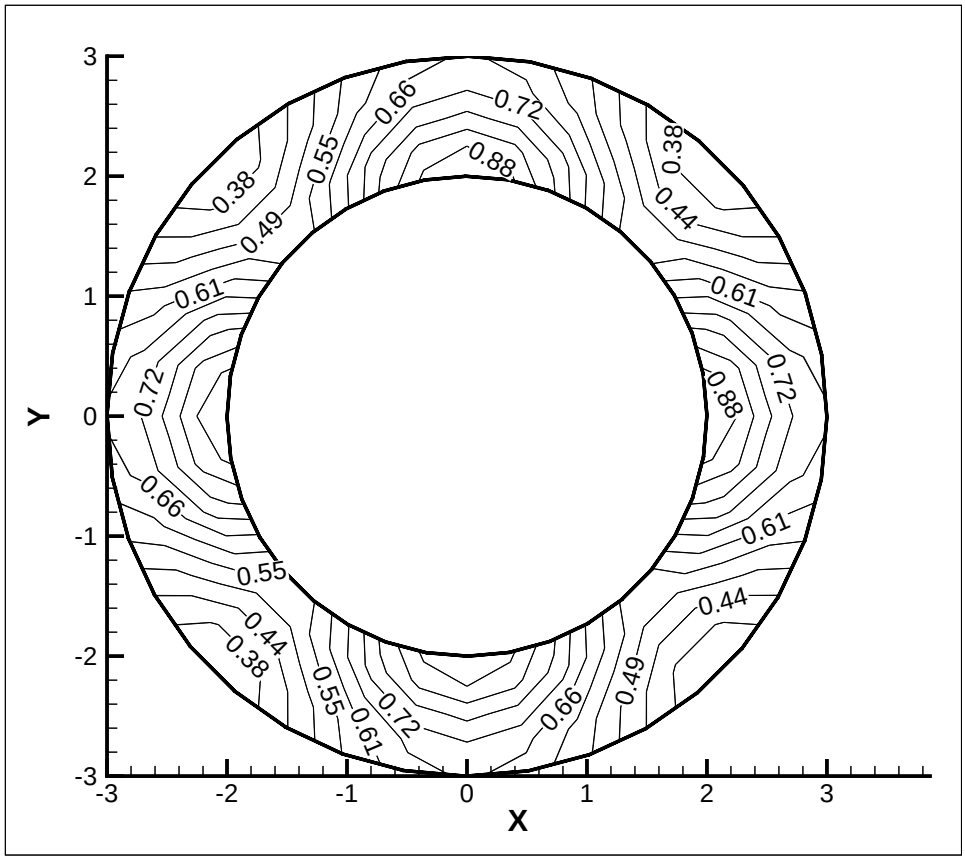

Figure 5: Inverse problem: computed normal stress magnitude when only outer boundary conditions were specified

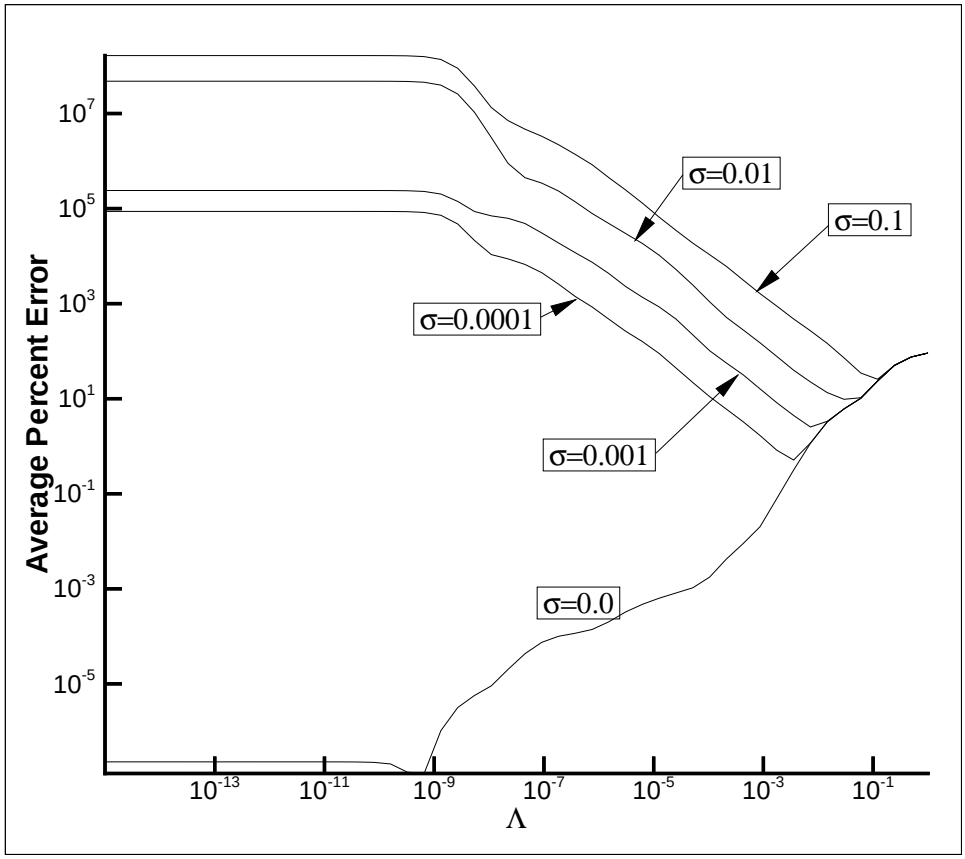

Figure 6: Average percent error of predicted temperatures on unknown boundaries for regularization method 1 for cylinder region

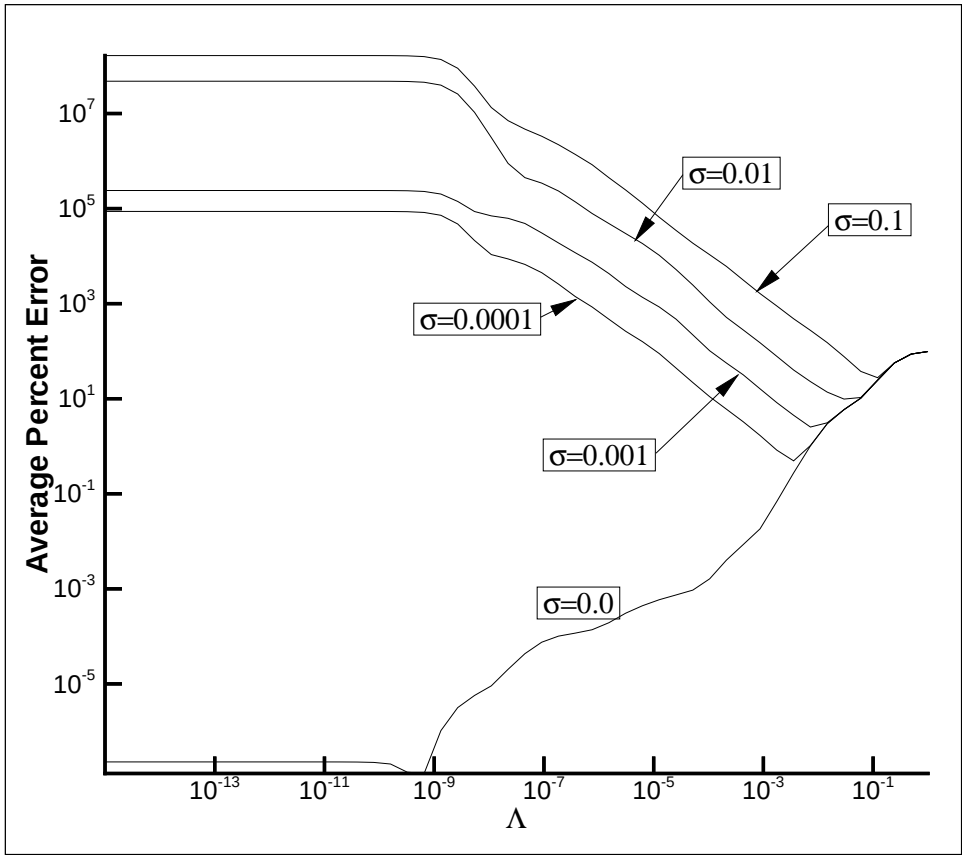

Figure 7: Average percent error of predicted temperatures on unknown boundaries for regularization method 2 for cylinder region

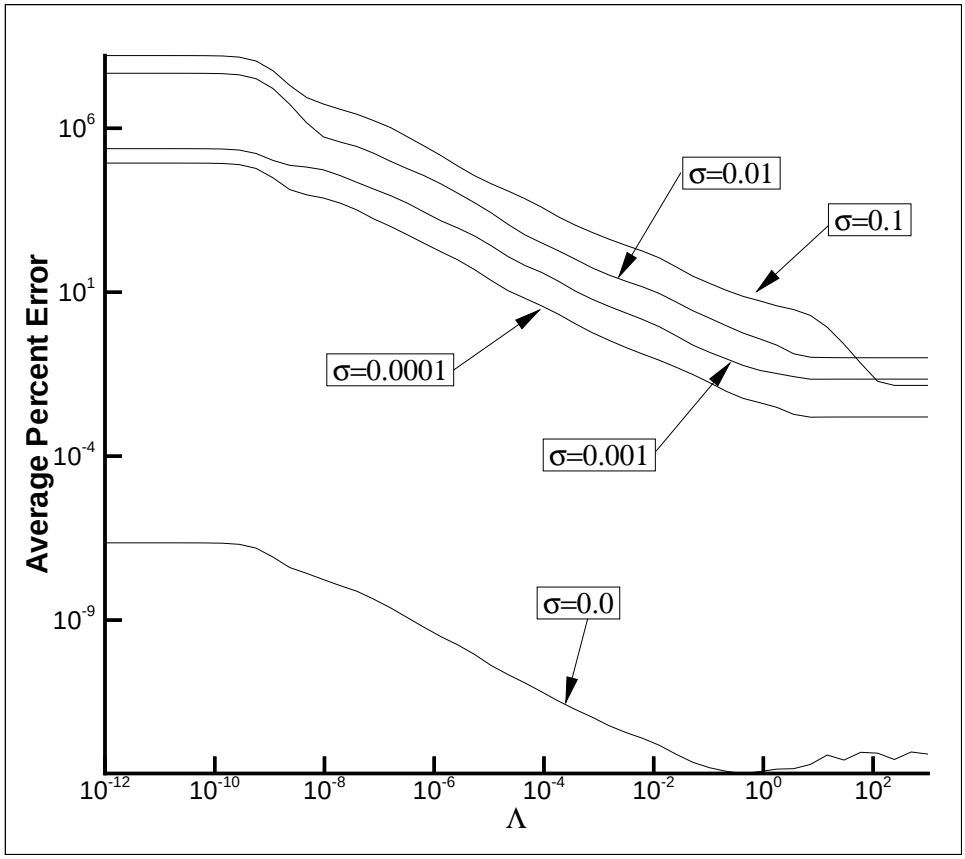

Figure 8: Average percent error of predicted temperatures on unknown boundaries for regularization method 3 for cylinder region

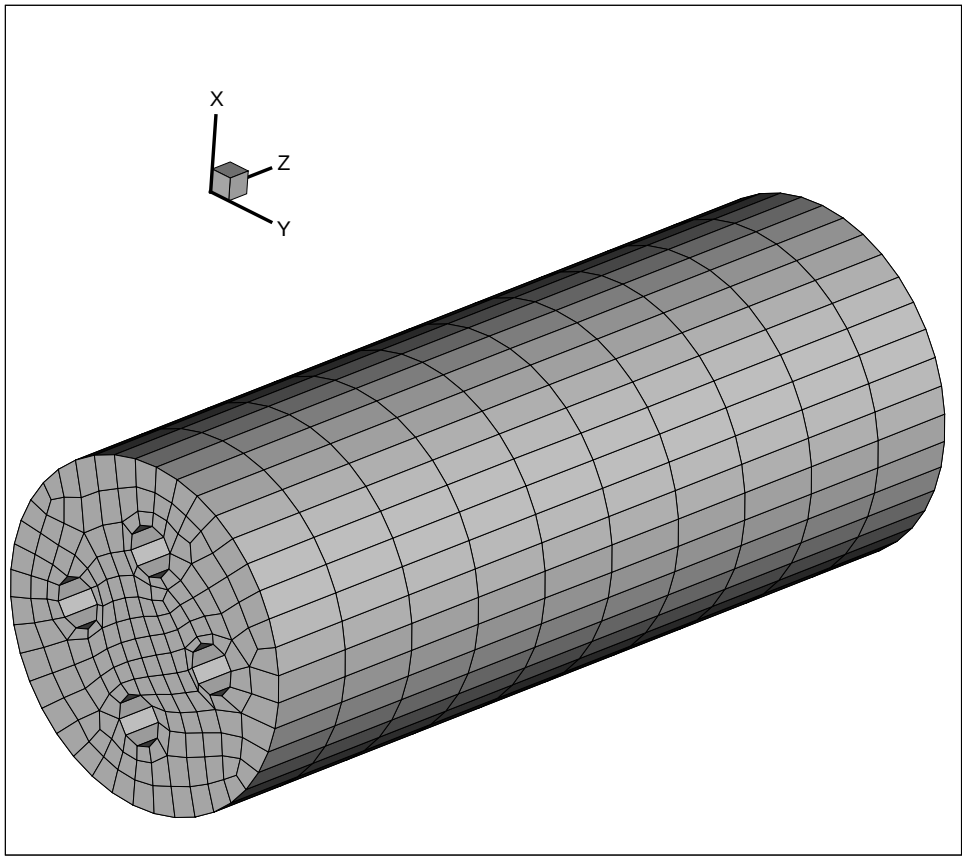

Figure 9: Surface mesh for multiply connected domain test case

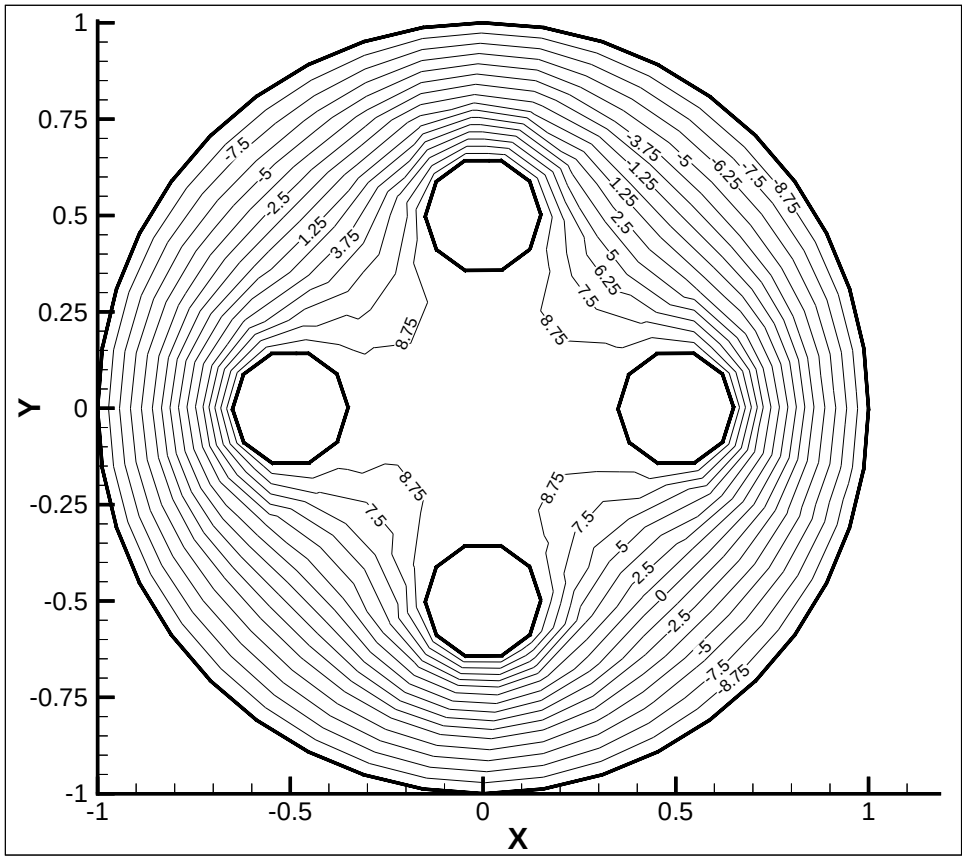

Figure 10: Direct problem: computed isotherms when both inner and outer boundary temperatures were specified

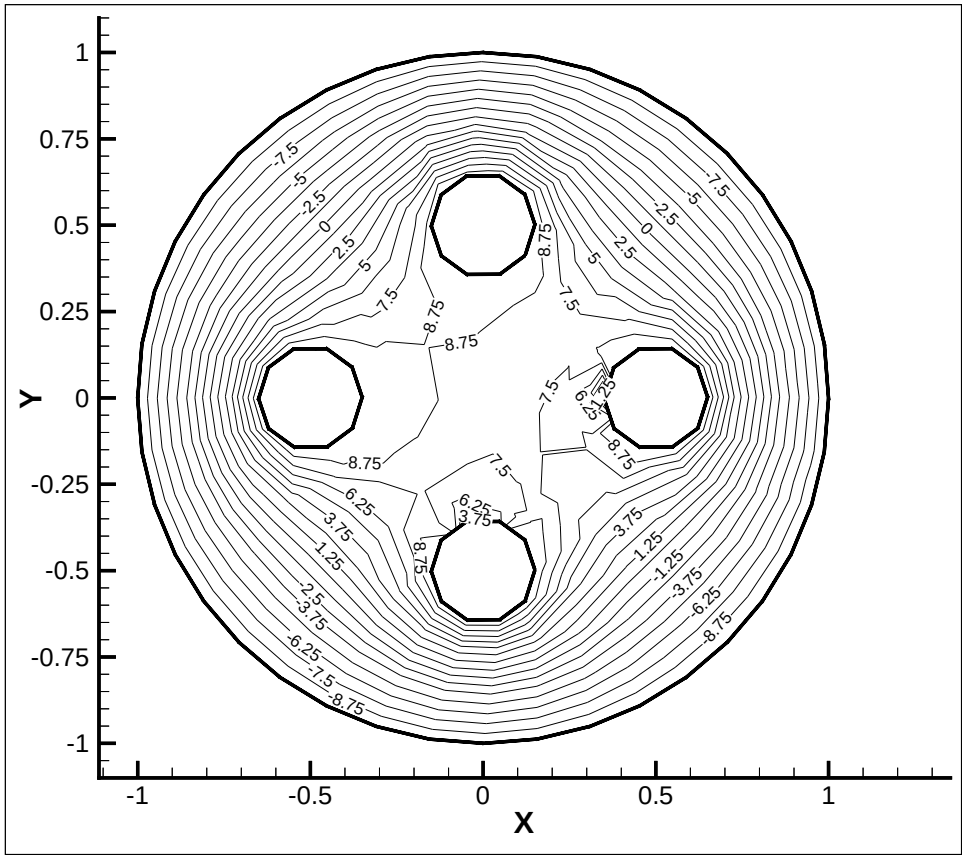

Figure 11: Inverse problem: computed isotherms when only outer boundary temperatures and fluxes were specified and using regularization method 1

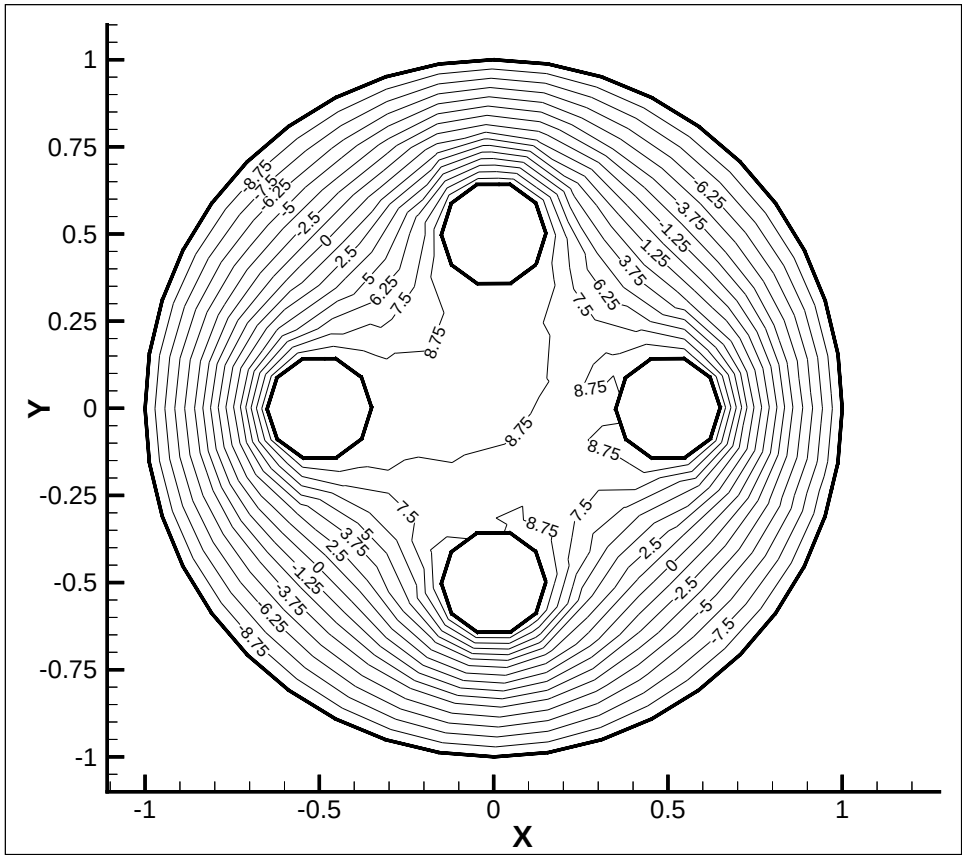

Figure 12: Inverse problem: computed isotherms when only outer boundary temperatures and fluxes were specified and using regularization method 2

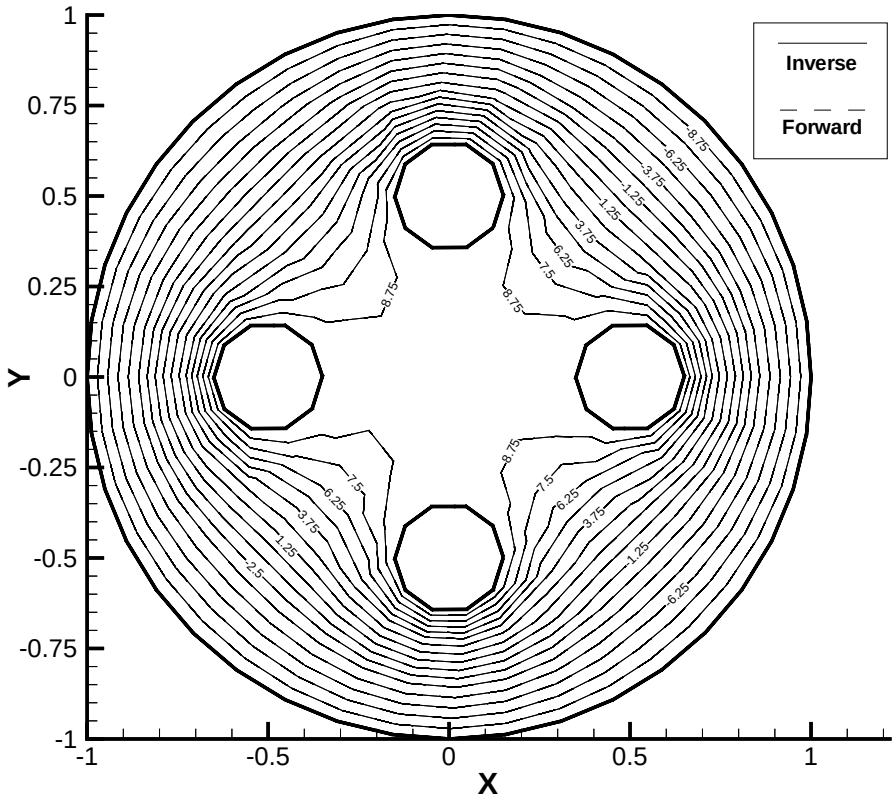

Figure 13: Inverse problem: computed isotherms when only outer boundary temperatures and fluxes were specified and using regularization method 3 (Inverse and Direct contours plotted together)

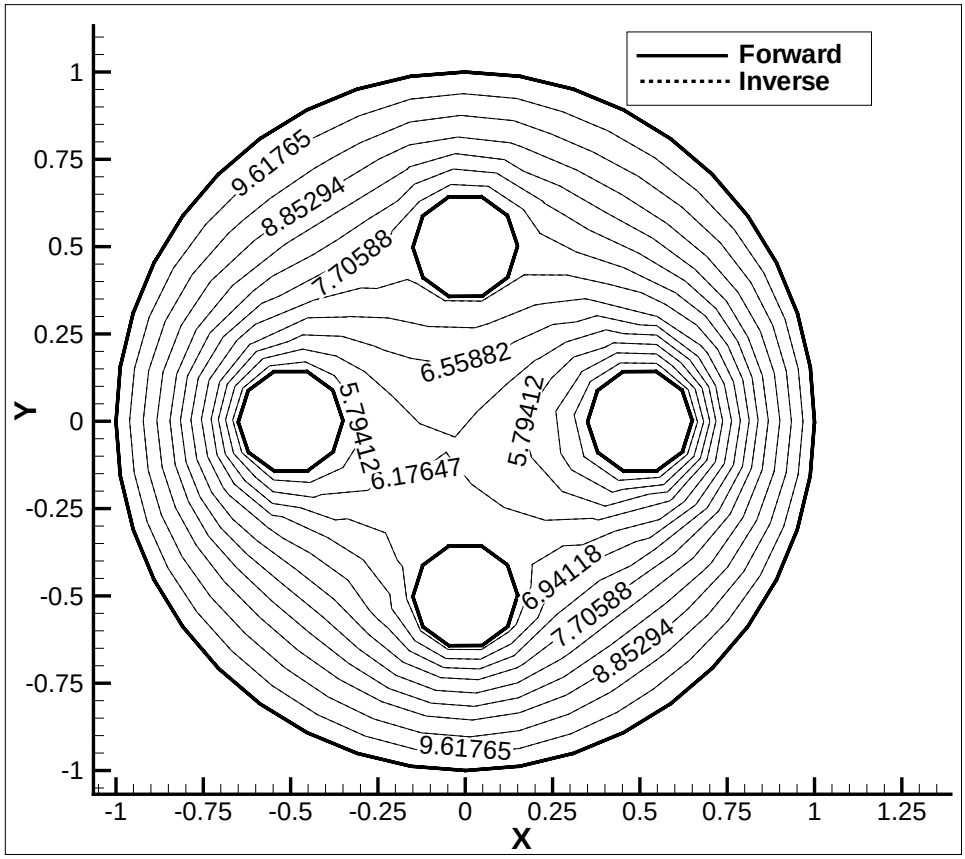

Figure 14: Inverse problem: computed isotherms on $x - y$ plane at $z = 0.5\ m$ when only outer boundary temperatures and fluxes were specified

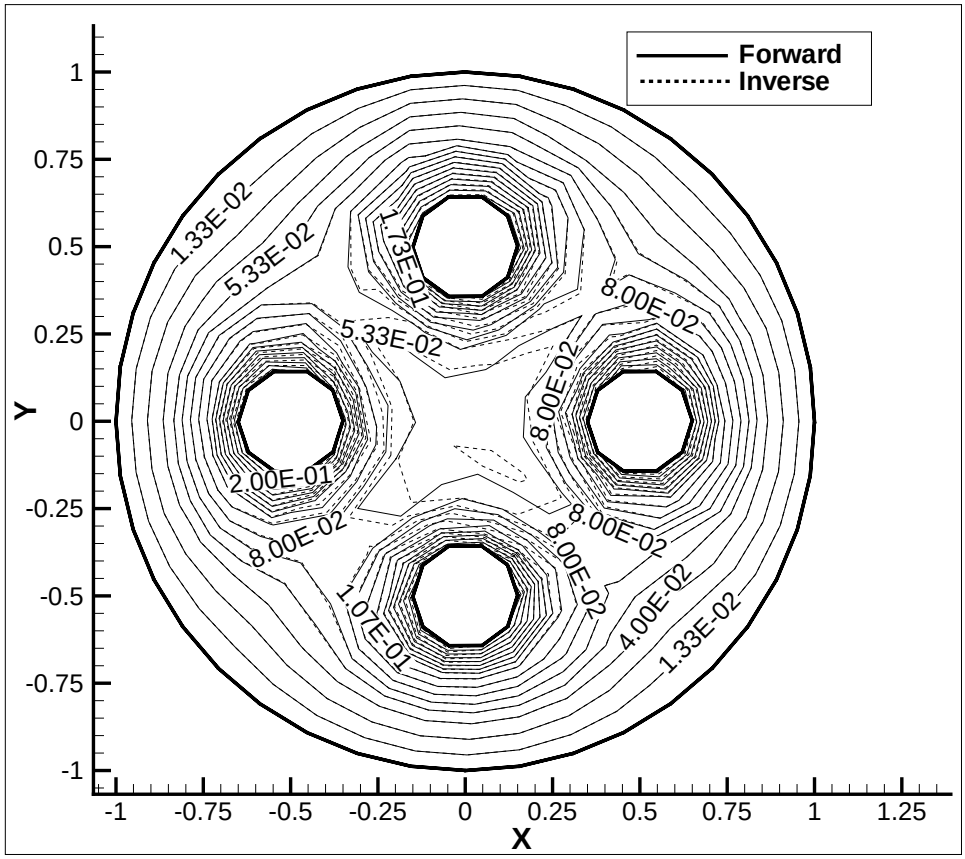

Figure 15: Inverse problem: computed displacement magnitude on $x-y$ plane at $z = 0.5\ m$ when only outer boundary displacements and tractions were specified

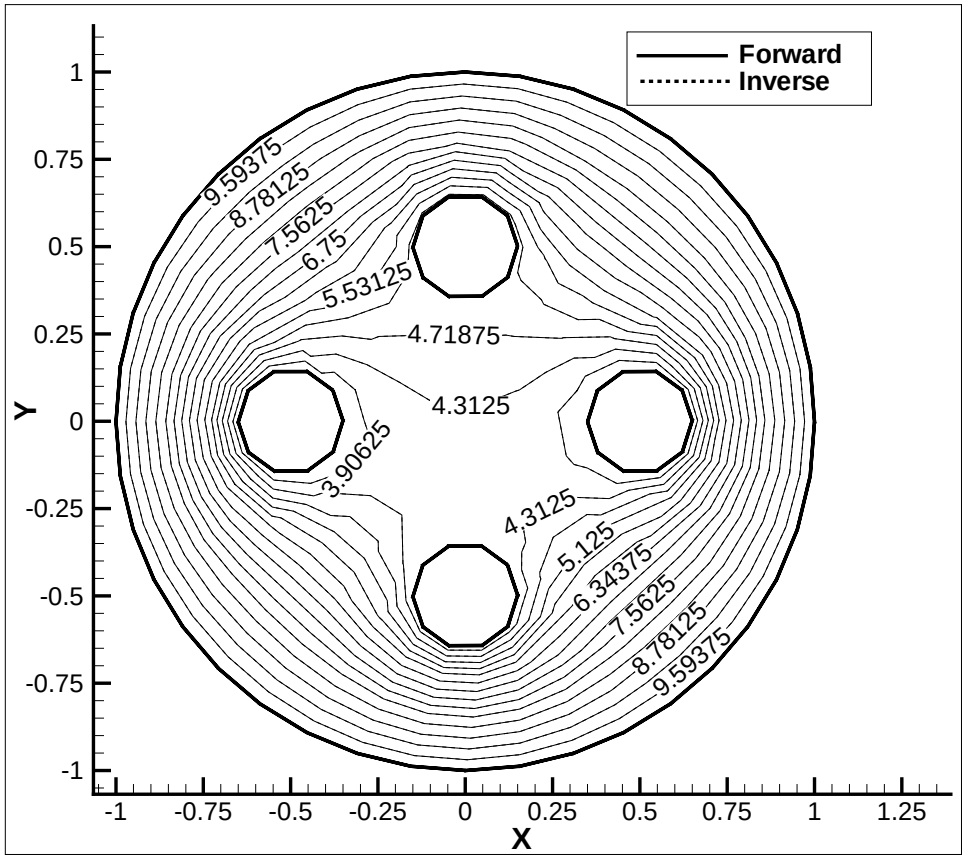

Figure 16: Inverse problem: computed isotherms on $x - y$ plane at $z = 2.5\ m$ when only outer boundary temperatures and fluxes were specified

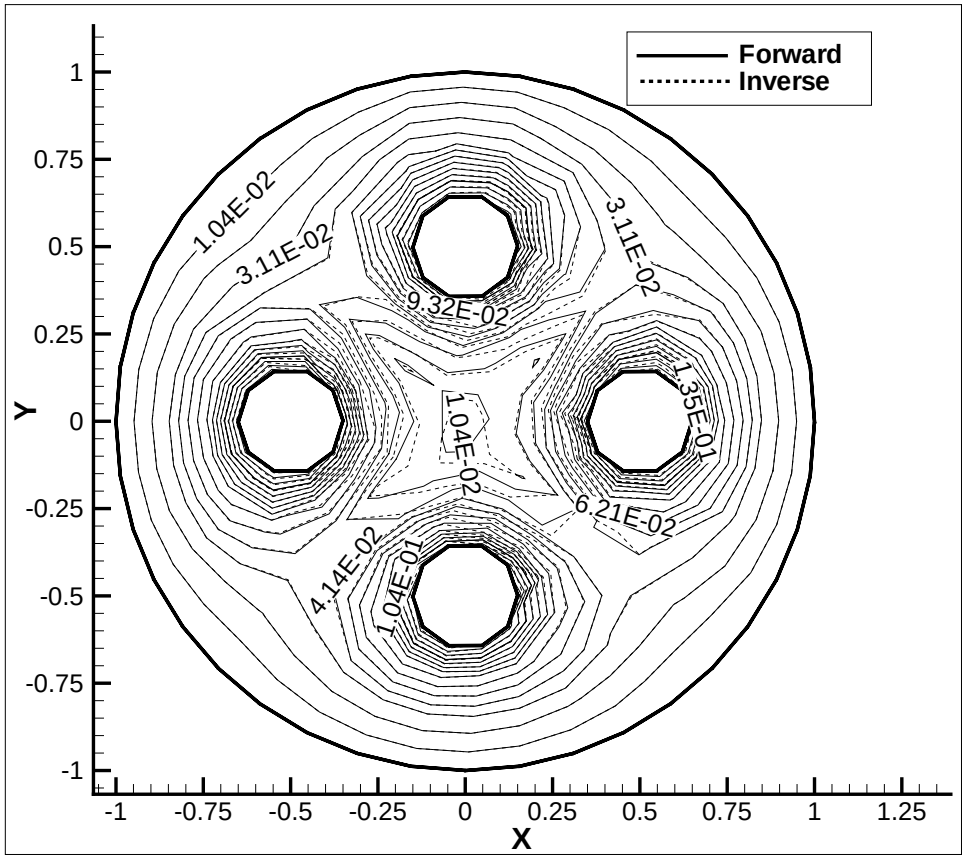

Figure 17: Inverse problem: computed displacement magnitude on $x-y$ plane at $z = 2.5\ m$ when only outer boundary displacements and tractions were specified

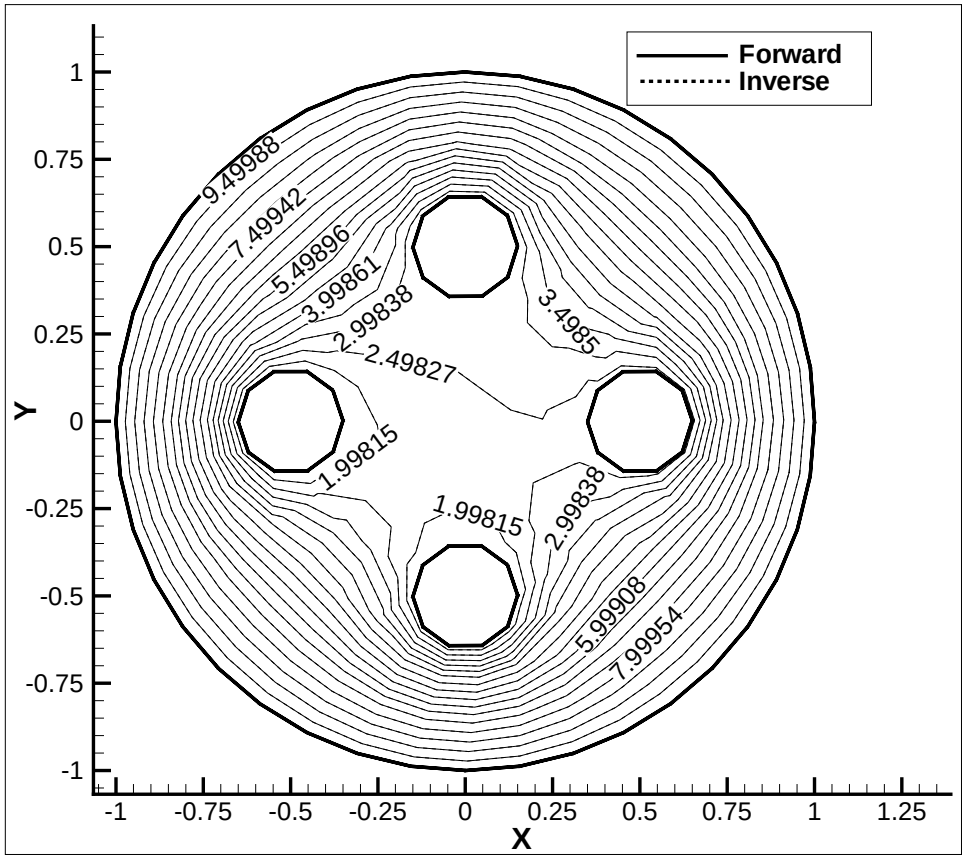

Figure 18: Inverse problem: computed isotherms on $x - y$ plane at $z = 4.5\ m$ when only outer boundary temperatures and fluxes were specified

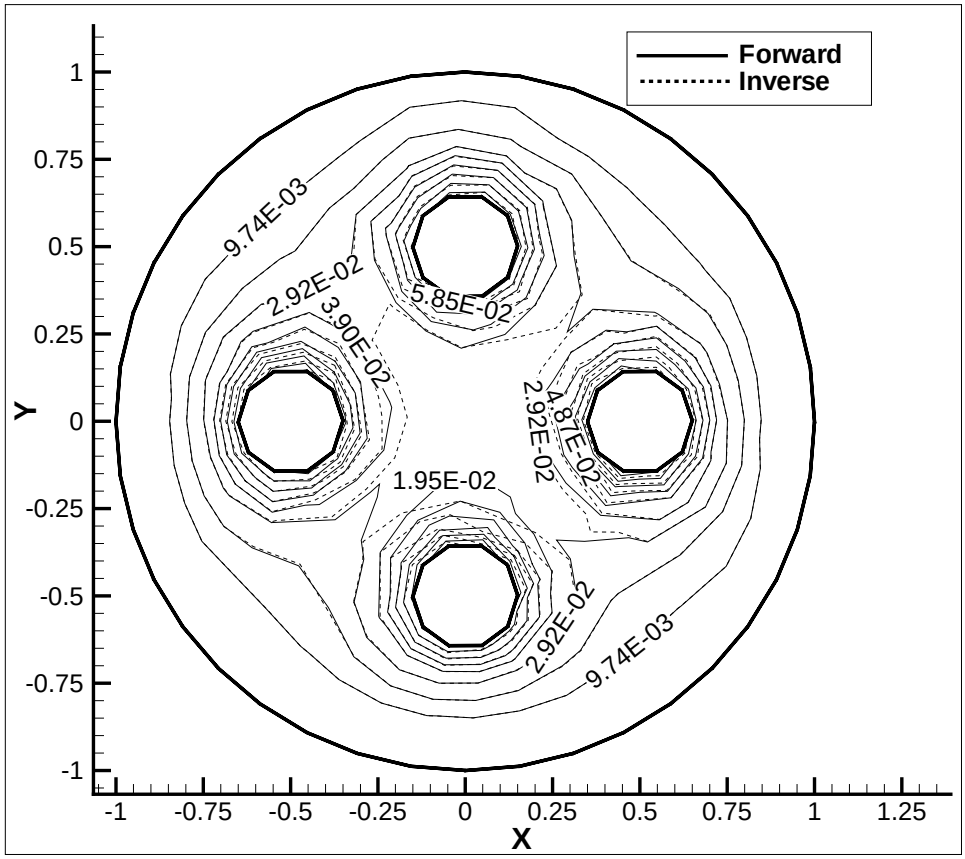

Figure 19: Inverse problem: computed displacement magnitude on $x-y$ plane at $z = 4.5\ m$ when only outer boundary displacements and tractions were specified